Interaction of Alzheimer β-Amyloid Peptide(1−40) with Lipid Membranes†

Evelyne Terzi,‡ Günter Hölzemann,§ and Joachim Seelig*,‡

Department of Biophysical Chemistry, Biocenter of the University of Basel, Klingelbergstrasse 70, CH-4056 Basel, Switzerland, and Merck KGaA, D-64271 Darmstadt, Germany

Received July 29, 1997; Revised Manuscript Received September 29, 1997⊗

ABSTRACT: The β-amyloid peptide βAP(1−40), a 40-amino acid residues peptide, is one of the major components of Alzheimer's amyloid deposits. βAP(1−40) exhibits only a limited solubility in aqueous solution and undergoes a concentration-dependent, cooperative random coil ⇄ β-structure transition for C_{pep} > 10 μM [Terzi, E., Hölzemann, G., and Seelig, J. (1995) *J. Mol. Biol. 252,* 633−642]. In the presence of acidic lipid, the equilibrium is shifted further toward β-structured aggregates. We have now characterized the lipid−peptide interaction using circular dichroism (CD) spectroscopy, lipid monolayers, and deuterium and phosphorus-31 solid-state nuclear magnetic resonance (NMR). CD spectroscopy revealed a distinct interaction between βAP(1−40) and negatively charged unilamellar vesicles. In addition to the random coil ⇄ β-structured aggregate equilibrium at low lipid-to-peptide (L/P) ratios, a β-structure → α-helix transition was observed at L/P > 55. βAP(1−40) was found to insert into acidic monolayers provided the lateral pressure was low (20 mN/m). The extent of incorporation increased distinctly with the content of acidic lipid in the monolayer. However, at a lipid packing density equivalent to that of a bilayer (lateral pressure ≥ 32 mN/m), no insertion of βAP(1−40) was observed. The lipid molecular structure in the presence of βAP(1−40) was studied with NMR. Phosphatidylcholine (PC) was selectively deuterated at the choline headgroup and at the *cis*-double bond of the oleic acyl chain and mixed with phosphatidylglycerol (PG). Phosphorus-31 NMR showed that the lipid phase retained the bilayer structure at all lipid-to-protein ratios. Deuterium NMR revealed no change in the headgroup conformation of the choline moiety or in the flexibility and ordering of the hydrocarbon chains upon the addition of βAP(1−40). It can be concluded that βAP(1−40) binds electrostatically to the outer envelope of the polar headgroup region without penetrating between the polar groups. The data suggest a new mechanism of helix formation induced by the proper alignment of five positive charges of βAP(1−40) on the negatively charged membrane template.

Alzheimer's disease is the predominant form of senile dementia and is characterized by neuritic plaques and cerebrovascular amyloid deposits. The core of the senile plaques consists of amyloid fibrils that give an X-ray diffraction pattern typical of ordered but not formally crystalline β-sheet structures. The major component of the amyloid core is the β-amyloid peptide (βAP),[1] a 39−43-residue polypeptide that is a cleavage product of a larger transmembrane amyloid precursor protein, APP (*1*−*3*).

Soluble, monomeric βAP appears to be a normal constituent of cerebrospinal fluid at subnanomolar concentrations (*4*−*6*). At higher concentrations under proper conditions of pH and salt concentration, βAP self-assembles into fibrils. *In vitro* studies with cell cultures have demonstrated that fibrillar βAP is toxic to neurons while monomeric βAP is not. The 'β-amyloid hypothesis' thus states that the excess deposition of βAP is somehow responsible for observed neurodegenerative changes observed *in vivo* (*7*−*9*).

However, the action mechanism of βAP and the causative role of βAP fibrils in particular are still obscure. Evidence in favor of βAP binding to several cell surface receptors has been presented. The serpin−enzyme complex receptor recognizes soluble, nontoxic β-amyloid peptide but not aggregated cytotoxic β-amyloid peptide (*10, 11*). It does not mediate the cytotoxic effect of aggregated βAP but could play a protective role by mediating clearance and catabolism of monomeric, soluble βAP. Selective binding of βAP fragments to the NK-1 tachykinin receptor has also been reported (*12*), but others have failed to show such interactions (*13*). Likewise, several studies have indicated the possibility that intracellular uptake of βAP is part of the toxic process. On the other hand, the majority of experimental data argue against an active accumulation of βAP in cells that are sensitive to the peptide (*1*).

Again another action mechanism of βAP is its ability to induce ionic conductance in lipid model membranes (*14*−*16*). Evidence has also been shown that βAP disrupts membranes containing acidic lipids (*17, 18*) and that the C-terminal domain of βAP has fusogenic properties (*19*). Whether or not the disruption of the cell membrane or the incorporation of βAP into the lipid bilayer could explain the observed neurotoxic effects has yet to be determined.

No high-resolution structure of amyloid-like plaques is available; in fact, the existence of a single, homogeneous structure is rather improbable (*20*). X-ray diffraction patterns of amyloid-like plaques reveal repeating structures that are

† Supported by the Swiss National Science Foundation Grant 31.42058.94.

* To whom correspondence should be addressed.

‡ University of Basel.

§ Merck KGaA.

⊗ Abstract published in *Advance ACS Abstracts,* November 15, 1997.

[1] Abbreviations: βAP, β-amyloid peptide; MOPS, 3-(*N*-morpholino)-propanesulfonic acid; POPC, 1-palmitoyl-2-oleoyl-*sn*-glycero-3-phosphocholine; POPG, 1-palmitoyl-2-oleoyl-*sn*-glycero-3-phosphoglycerol; TFE, trifluoroethanol; CD, circular dichroism; NMR, nuclear magnetic resonance.

S0006-2960(97)01843-6 CCC: $14.00

usually interpreted in terms of antiparallel peptide chains forming a β-pleated sheet. This is supported by X-ray diffraction studies of βAP fibrils derived from various βAP fragments (*21*). However, the β-sheet structure derived from globular proteins may bear little resemblance to the amyloid secondary structure (*20*). Distance measurements with solid-state NMR have revealed an unusual structure, probably involving a *cis*-amide bond, in aggregated βAP model peptides (*22*). This structure is incompatible with the conventional cross-β-fibrillar structure derived from silk and usually implied for amyloid-like plaques.

By definition, amyloid-like plaques are insoluble in water. Many spectroscopic studies have thus been performed in the presence of nonpolar solvents, using either trifluoroethanol (TFE)/water mixtures or sodium dodecyl sulfate (SDS) micelles (*23*−*25*). Under these conditions, βAP and most of its fragments are monomeric and adopt an at least partially α-helical conformation. Since TFE and SDS are considered as membrane-mimicking solvents, it has thus been suggested that βAP and some of its fragments penetrate into lipid membranes as α-helical monomers. In particular, the fragment βAP(25−35) has been suggested to be highly lipophilic and to insert into the membrane hydrophobic core (*26*). Other peptides have been predicted to insert in an oblique way into the lipid membrane or parallel or perpendicular to it (*19*).

The peptide conformation in TFE/water and SDS/water mixtures must be contrasted with that in the absence of organic solvents. βAP and some of its fragments exhibit a limited solubility in the micromolar range (in the absence of salt). ^{1}H-NMR (*27*) and CD spectroscopy (*28*−*30*) demonstrate that the conformation of βAP in the aqueous phase is different from the α-helical conformation induced by TFE or SDS. The ^{1}H-NMR data of βAP(1−25) NH_2 indicate a flexible structure with several turns and at least two short strands (*27*). Likewise, CD spectra of βAP(1−40) and βAP(25−35) reveal a random coil structure at low peptide concentrations ($C_{pep} < 30\ \mu$M) and a concentration-dependent random coil $\rightleftarrows$ β-structured aggregate transition at higher concentrations (*28, 30*). The latter transition can be influenced by the presence of lipid membranes. At a given peptide concentration, the addition of negatively charged lipid vesicles shifts the conformation from random coil to 40−60% β-structure (*29, 30*).

Different experimental procedures thus induce different βAP structures, i.e., (i) α-helical conformation in TFE and SDS micelles, (ii) essentially random coil structure with β-turns in aqueous solution at low peptide concentrations, and (iii) β-structured aggregates in solution and in contact with lipid membranes. Since the interrelationship between the α-helical conformation in membrane-mimicking solvents and the potential of βAP to penetrate into lipid membranes is not clear, we have investigated this problem with different physical−chemical techniques. We have measured the conformational changes of βAP as a function of the lipid concentration and composition with CD spectroscopy. Using the monolayer technique, we have quantitatively characterized the penetration of βAP into neutral and charged lipid monolayers at different surface pressures. Finally, the effect of βAP on the lipid molecular structure was monitored with solid-state deuterium and phosphorus-31 NMR in combination with selectively deuterated lipid molecules.

MATERIALS AND METHODS

Materials. βAP(1−40) was purchased from Saxon Biochemicals GmbH (Hannover, Germany). The purity of the peptide was checked by HPLC (better than 97% purity). The peptide has the amino acid sequence:

DAEFRHDSGYEVHHQKLVFFAEDVGSNKGAIIG-LMVGGVV

Its structure was confirmed by electrospray mass spectrometry. Lyophilized peptide was dissolved in the appropriate amount of 10 mM MOPS or Tris buffer at pH 7.4. The peptide solutions were equilibrated by stirring for 1−2 h at room temperature.

1-Palmitoyl-2-oleoyl-*sn*-glycero-3-phosphocholine (POPC) and 1-palmitoyl-2-oleoyl-*sn*-glycero-3-phosphoglycerol (POPG) were purchased from Avanti Polar Lipids (Birmingham, AL) and used without further purification.

For NMR measurements, POPC was selectively deuterated at the α or β segment of the choline headgroup as described previously (*31*). The following nomenclature for the head group segments was used:

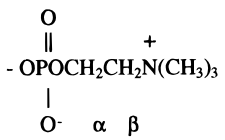

1-palmitoyl-2-[9′,10′-$^2H_2$]oleoyl-*sn*-glycero-3-phosphocholine ([9′,10′-$^2H_2$]-POPC) was prepared as described by Seelig and Waespe−Sarcevic (*32*).

Preparation of Lipid Samples. For CD experiments, small unilamellar vesicles of ∼30 nm diameter were prepared as follows. POPC and POPG were dissolved in chloroform (20 mg/mL) and were mixed in the appropriate molar ratio. The solvent was evaporated under a nitrogen stream leading to a thin lipid film, which was dried under vacuum overnight. Buffer was added to the dry lipid film (∼40 mg) leading to a final lipid concentration of ∼55 mM. The lipid dispersion was vortexed and then sonicated under a nitrogen atmosphere for about 10 min (at 10 °C) until an almost clear solution was obtained. Metal debris from the titanium tip was removed by centrifugation in an Eppendorf centrifuge at 14000 rpm for 5 min.

For NMR measurements, deuterated POPC and non-deuterated POPG were mixed in chloroform in the appropriate molar ratio (total of 10 mg of lipid). The organic solvent was evaporated under nitrogen, and the resulting thin film of lipid was dried under vacuum overnight. The lipids were dispersed in 10 mL (or 1.1 mL) of buffer containing the appropriate amount of βAP(1−40) added as aliquots from a 25 μM (or 0.1 mM) stock solution. Multilamellar vesicles were formed by vortexing and eight freeze−thaw cycles. The samples were centrifuged for 2 h at 120000*g*. The pellets were used for ^{2}H- and ^{31}P-NMR.

Circular Dichroism Spectroscopy. CD measurements were carried out on a Jasco J720 spectropolarimeter. All measurements were performed at room temperature. The path length of the quartz cell was 1 mm or 0.1 mm. All spectra were corrected by subtracting the buffer baseline.

For membrane-binding studies, sonified unilamellar vesicles of defined lipid composition were added to a buffered peptide solution and were measured after 10-min equilibration time.

The secondary structures of the peptide was estimated from spectral simulations based on reference CD spectra of Yang et al. (*33*), included in the Jasco J720 software. Results are expressed in terms of mean residue ellipticity $[\Theta]_{MR}$ (deg cm^2 dmol^{-1}).

NMR Measurements. All spectra were recorded on a Bruker-Spectrospin MSL 400 spectrometer operating at a frequency of 61.4 MHz for ^{2}H-NMR and 162 MHz for ^{31}P-NMR. For the deuterium NMR measurements, the quadrupole echo technique was employed with full-phase cycling. The 90° pulse was 4.45 μs, the interpulse delay was 45 μs, and the recycle delay 250 ms. The spectral width was 50 kHz for headgroup studies and 125 kHz for studies of the hydrocarbon region.

The ^{31}P spectra were recorded using the Hahn-echo sequence with gated proton decoupling and phase cycling. The 90° pulse was 2.55 μs, the echo spacing was 45 μs, the recycle delay was 2 s, and the spectral width was 50 kHz. The chemical shielding anisotropy was measured between the edges of the spectrum at half-height of the low-field shoulder. The error was estimated to be ±1 ppm.

Monolayer Measurements. The surface pressure was measured by the Wilhelmy method, using a monolayer apparatus consisting of a round Teflon trough with a total area of 362 cm^2 divided into eight compartments (Type RMC2-T, Mayer Feintechnik, Göttingen, FRG) (*34*). A mixed POPC/POPG or pure lipid monolayer was formed by spreading a lipid solution in *n*-hexane/ethanol (9/1, v/v) onto the aqueous phase. The monolayer was stabilized at a preset surface pressure, which was kept constant throughout the experiment by an electronic feedback system. Small amounts of a 0.1 mM stock solution of β-AP(1−40) were injected into the buffer subphase. Measurements were performed at room temperature.

RESULTS

Circular Dichroism Spectroscopy of β-AP(1−40). β-AP(1−40) dissolved in buffer (pH 7.4) at concentrations below 25 μM adopts a random coil conformation. Increasing the peptide concentration from 25 to 100 μM leads to a cooperative random coil ⇄ β-structure transition (*30*). In contrast, an α-helical structure is induced if β-AP is dissolved in organic solvents such as trifluoroethanol or if incorporated into micelles (SDS, octylglucoside) (*23*−*25*). Again a different situation is encountered with lipid membranes. Addition of charged POPC/POPG vesicles (75/25) (but not neutral POPC vesicles) to solutions of β-AP(25−35) and β-AP(1−40) in the random coil conformation induced a transition to a β-structure (*29, 30*). A similar random coil ⇄ β-structure transition was observed in the present study upon addition of pure POPG vesicles to a solution of β-AP(1−40). As shown in Figure 1, a 25 μM β-AP(1−40) solution was titrated with sonified POPG vesicles (55 mM). In the initial titration steps, the addition of POPG induces first a random coil ⇄ β-structure transition. At a lipid-to-peptide molar ratio of ∼11 (Figure 1, curve 2), the β-AP(1−40) CD spectrum reveals a structure with about 40−60% β-sheet content. The α-helix content is negligible. However, upon further addition of sonified POPG vesicles, a second change in the CD spectra can be noted, indicating the formation of an α-helical structure (Figure 1, curves 3−5).

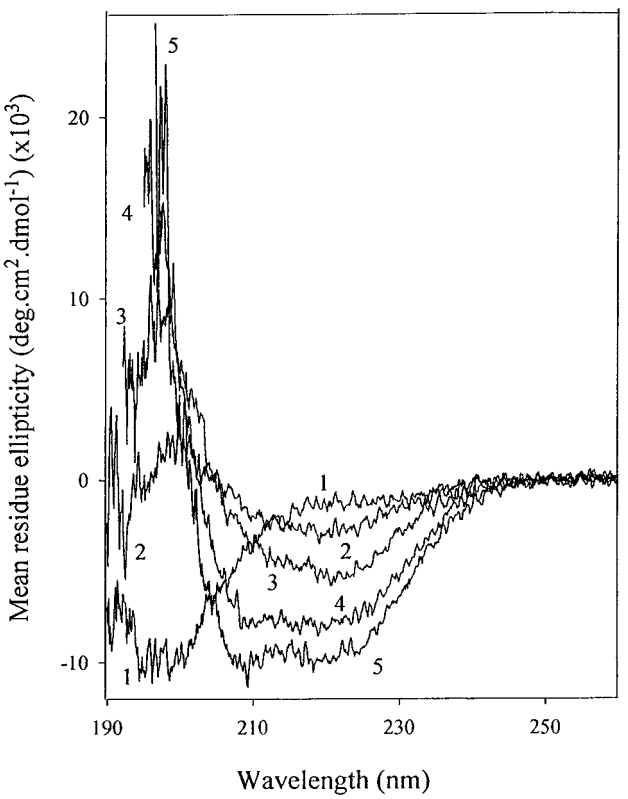

FIGURE 1: Lipid-induced conformational change of β-AP(1−40) dissolved in 10 mM Tris at pH 7.4. A 25 μM β-AP solution was titrated with sonified unilamellar vesicles of POPG 100% (lipid concentration: 55 mM). The CD spectra correspond to different molar lipid-to-peptide ratio. Curve 1, L/P = 0; 2, 11; 3, 22; 4, 55; 5, 110.

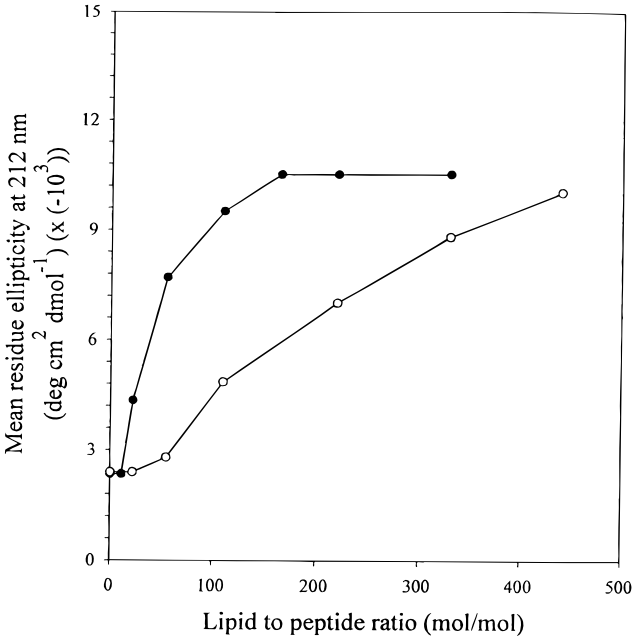

FIGURE 2: Lipid-induced β-sheet to α-helix transition of β-AP(1−40). The ellipticity increase at 212 nm is shown as a function of the molar lipid-to-peptide ratio. β-AP(1−40) (at a concentration of 25 μM in 10 mM Tris pH 7.4) was titrated with sonified unilamellar vesicles of POPG 100% (●) and of POPC/POPG (75/25 mol/mol) (○) (lipid concentration: 55 mM).

Figure 2 summarizes the variation of the α-helix content with the lipid-to-protein ratio as reflected in the change in CD intensity at 212 nm. For pure POPG vesicles, the β-structure ⇄ α-helix transition starts at L/P ≈ 11 and is

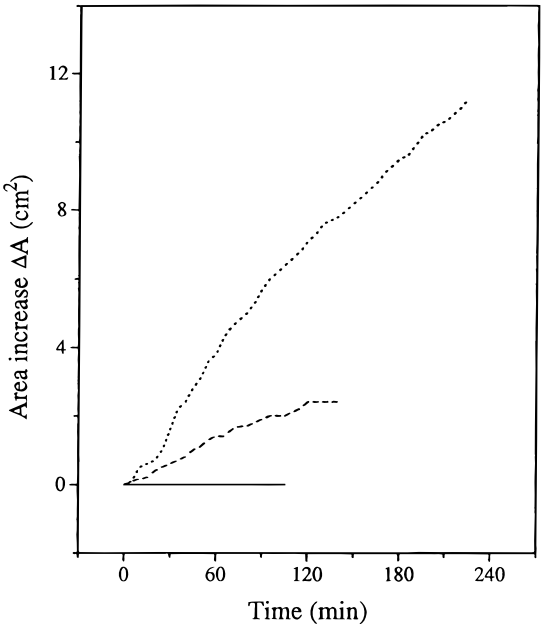

FIGURE 3: Area increase, ΔA, of lipid monolayers induced by the insertion of βAP(1−40) (0.5 μM) as a function of time (measuring temperature 22 ± 1 °C). The monolayers were spread on buffer solution (10 mM Tris buffer adjusted to pH 7.4. (···) 100% POPG monolayer compressed at a lateral pressure of 20 mN/m. (- - -) POPC/POPG (37.5/62.5 mol/mol) monolayer at 20 mN/m. (—) POPC/POPG (75/25 mol/mol) monolayer at 32 mN/m.

finished within a narrow interval. A maximum of ∼39% α-helix is reached at a lipid-to-peptide molar ratio of 165. The remaining structural elements are 29% β-turn and 32% random coil as judged from computer simulations of the CD spectra.

For POPC/POPG (75/25) vesicles, which mimick more closely the electric charge density of biological membranes than pure POPG vesicles, the α-helix content rises gradually for L/P > 55. At a lipid-to-peptide molar ratio of 440, about the same maximum α-helix content is obtained as with pure POPG vesicles at L/P = 165.

Insertion Studies of βAP(1−40) Using Lipid Monolayers. Lipid monolayers have proven to be a sensitive tool to study lipid−peptide and lipid−protein interactions (*35*, *36*). The method can be employed with the lipid film kept at constant area or at constant pressure. In the second mode, as employed here, the monolayer pressure is kept constant at a preset value by an electronic feedback system, and the area increase upon peptide penetration is recorded with a movable barrier. The area increase is proportional to the number of penetrating molecules.

Monolayers were formed by spreading a lipid solution of defined POPC/POPG composition in hexane/ethanol (9:1 v/v) onto the buffer phase at pH 7.4. A small amount of a βAP-(1−40) stock solution was injected into the subphase, yielding a peptide concentration of 0.5 μM. The resulting area change, Δ*A*, upon peptide penetration was recorded. Figure 3 displays the time course of the area increase, Δ*A*, for two monolayers with different contents of negatively charged lipid at a pressure of 20 mN/m. The insertion of βAP(1−40) is a rather slow process for both monolayers. This is in contrast to most other drugs and peptides that have been studied so far (cf. refs 37 and 38). For the POPC/POPG (37.5/62.5) membrane, a plateau value is reached after about 2 h, and the relative area increase, Δ*A*/*A* is about 10%

Table 1: Relative Area Increase (Δ*A*/*A*) Measured at Different Surface Pressures and for Various Lipid Compositions

lipid composition (mol/mol)	surface pressure (mN/m)	Δ*A*/*A* (%)	peptide conc (μM)
POPC 100%	20	4.8	0.5
POPC/POPG (75/25)	20	4.0	0.5
POPC/POPG (50/50)	20	4.8	0.5
POPC/POPG (50/50)	20	9.2	0.5
POPC/POPG (37.5/62.5)	20	10.6	0.5
POPC/POPG (31/69)	20	21.3	0.5
POPC/POPG (25/75)	20	39.1	0.5
POPG 100%	20	>43.1	0.5
POPC/POPG (25/75)	24	0	0.5
POPC/POPG (50/50)	32	0	0.5
POPC/POPG (75/25)	32	0	7.9

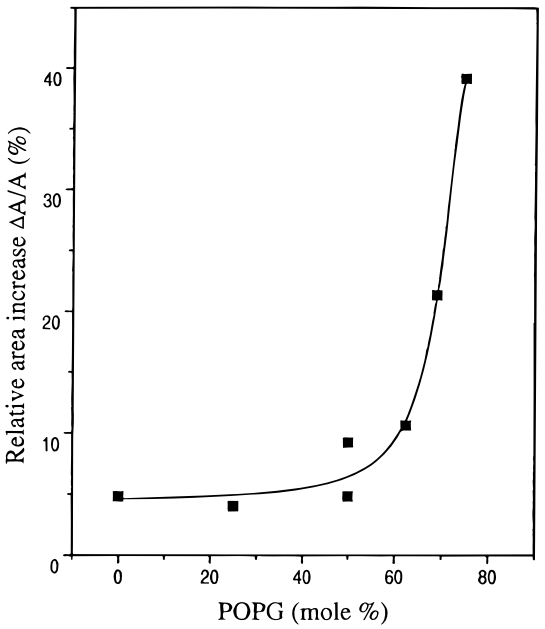

FIGURE 4: Relative area increase Δ*A*/*A* due to insertion of βAP-(1−40) (0.5 μM) as a function of negatively charged lipid content. The monolayer was kept at a constant lateral pressure of 20 mN/m and was spread on 10 mM Tris buffer at pH 7.4.

(cf. Table 1). For a pure POPG monolayer the area expansion was more pronounced; however, no stable plateau was reached within the measuring period of ∼3 h.

Figure 4 summarizes the insertion of βAP(1−40) (0.5 μM) into mixed POPC/POPG monolayers (at 20 mN/m) as a function of the PG content. In the range of 0−50% POPG, the incorporation of peptide is weak but increases almost exponentially above 50% POPG content.

A lateral pressure of 20 mN/m corresponds to a rather loose packing of the phospholipids, comparable to that in a micelle. Micellar solutions of sodium dodecyl sulfate and octylglucoside have indeed been shown to interact with βAP-(1−42) and to induce conformational changes of the peptide (*39*). A lateral pressure of 20 mN/m is, however, distinctly lower than the monolayer−bilayer equivalence pressure, which has been established as 32 mN/m by several methods (*37*). At this pressure, the lipid packing density in the monolayer is assumed to be comparable to that in the bilayer. We have therefore performed additional measurements at 32 mN/m. The time course for βAP(1−40) penetration into a POPC/POPG (75/25) monolayer is included in Figure 3, and further data are Summarized in Table 1. It can be concluded that βAP(1−40) cannot penetrate into mixed POPC/POPG

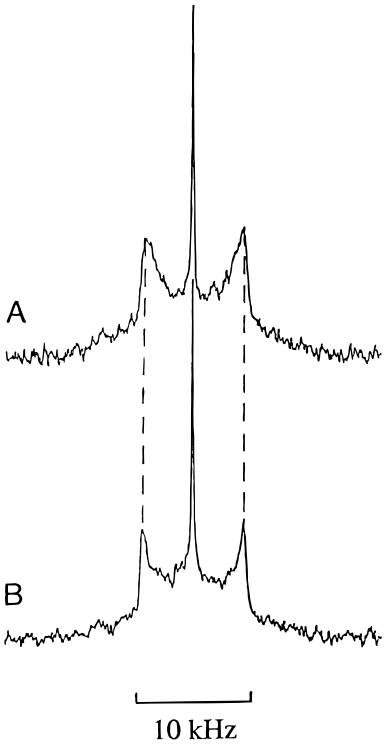

FIGURE 5: Deuterium NMR spectra of POPC/POPG (75/25 mol/mol) multilamellar liposomes without (A) and with (B) βAP(1−40). POPC was deuterated at the α-segment of the choline moiety (-NCH_2-CD_2OP-). The molar lipid-to-protein ratio in panel B was 55. Almost identical spectra were obtained at L/P ratios of 200 and 440. The multilamellar vesicles were prepared in MOPS buffer at pH 7.4. The sharp isotropic line results from natural abundance deuterium in water. The quadrupole splitting in the presence of βAP(1−40) was 9.3 ± 0.2 kHz; that in the absence of peptide was 8.9 ± 0.2 kHz.

monolayers when pressurized at the monolayer−bilayer equivalence pressure even at high content of POPG. This provides a first evidence that βAP(1−40) may not insert spontaneously into lipid bilayers and that a micellar environment is a rather poor model system to study βAP−lipid bilayer interactions.

Deuterium and Phosphorus-31 Magnetic Resonance. The interaction of βAP(1−40) with the phospholipid molecules was studied with phosphorus-31 and deuterium magnetic resonance. The phosphorus-31 NMR spectra (not shown) had the shape and the quantitative parameters previously reported for multilamellar phospholipid dispersions (*40, 41*). The maximum chemical shielding anisotropy was −45.7 ppm and was identical with and without βAP(1−40) at lipid-to-protein ratios between 55 and 400. It was also not possible to distinguish between the PC and the PG headgroups.

In a second type of experiment, POPC was selectively deuterated at the α- or β-segment of the choline headgroup and was mixed with non-deuterated POPG. Multilamellar lipid dispersions were formed with and without βAP(1−40) in the dispersing buffer (cf. Materials and Methods). Figure 5 shows deuterium NMR spectra of α-CD_2-POPC/POPG (75/25 mol/mol) membranes without βAP(1−40) (panel A) and at a lipid-to-protein ratio of 55 (panel B). Almost identical spectra are obtained. The central isotropic resonance is caused by the natural abundance of deuterium in water. Otherwise, the deuterium NMR spectra are characteristic of liquid-crystalline bilayers in which the headgroups execute rotationally symmetric motions around the bilayer normal

Table 2: Quadrupole Splitting $\Delta\nu_Q$ Deduced from ^{2}H-NMR Spectra of Mixed POPC/POPG Vesicles with and without βAP(1−40)

lipid composition (mol/mol)	lipid-to-peptide ratio (mol/mol)	quadrupole splitting $\Delta\nu_Q$ (kHz)
α-CD_2-POPC/POPG (75/25)	no peptide	8.9
α-CD_2-POPC/POPG (75/25)	55	9.4
α-CD_2-POPC/POPG (75/25)	200	9.2
α-CD_2-POPC/POPG (75/25)	400	9.3
α-CD_2-POPC/POPG (50/50)	no peptide	10.1
α-CD_2-POPC/POPG (50/50)	440	10.3
β-CD_2-POPC/POPG (75/25)	no peptide	2.4
β-CD_2-POPC/POPG (75/25)	440	2.4
9′,10′-d_2-POPC/POPG (75/25)	no peptide	(9′)13.0 (10′)1.9
9′,10′-d_2-POPC/POPG (75/25)	440	(9′)13.1 (10′)2.1

(*42*). The characteristic parameter of these spectra is the quadrupole splitting $\Delta\nu_Q$ as defined by the separation of the most intense peaks in the spectrum. $\Delta\nu_Q$ is a measure of the ordering and average orientation of the labeled headgroup segment. Inspection of Figure 5 reveals very similar quadrupole splittings with and without βAP(1−40). Identical results were obtained for other L/P ratios and also for β-CD_2-POPC/POPG (75/25 mol/mol) membranes. The membrane composition and the corresponding quadrupole splittings are summarized in Table 2. Taken together, the deuterium and phosphorus-31 NMR data demonstrate that βAP(1−40) is not involved in direct molecular interactions with the POPC headgroup.

This result is surprising since previous investigations have shown that the quadrupolar splittings of the choline headgroup are very sensitive to the presence of charged species such as ions (*43*−*45*), local anesthetic and drugs (*46*−*48*), charged phospholipids and surfactants (*49*−*51*), and peptides (*52*−*54*). The effect of charge on the choline headgroups causes a reorientation of the choline dipole (*55*). The only known exception is pentalysine, which shows no effect on the PC headgroup splittings in mixed PC/PS membranes (*56*). The binding of Lys_5 is purely electrostatic and could serve as a model to explain the present data with βAP(1−40) (cf. below).

Finally, we have also investigated the effect of βAP(1−40) on the hydrocarbon chain region of the lipid bilayer by employing POPC deuterated at the *cis*-double bond of the unsaturated hydrocarbon chain. Addition of cholesterol (*57*) or amphiphilic drugs that penetrate into the lipid membrane (*48*) lead to distinct changes in the quadrupole splittings of the *cis*-double bond. In the presence of βAP(1−40), no change in the quadrupole splittings was observed (cf. Table 2). It should be noted that quite different quadrupole splittings are observed for the C-9 and the C-10 segment of oleic acyl chain, but both splittings remained approximately constant upon the addition of βAP(1−40). Deuterium NMR thus demonstrates that βAP(1−40) does not penetrate into the bilayer interior, supporting the monolayer results.

DISCUSSION

The interaction of βAP(1−40) with lipid monolayers and lipid bilayers follows a surprising pattern, and the results obtained with different techniques appear to be contradictory at first sight. CD spectroscopy provides evidence for a conformational change of the peptide molecules induced by negatively charged lipid vesicles. In contrast, deuterium and phosphorus NMR reveal no conformational change of the lipid molecules in the presence of βAP(1−40), neither at

the level of the headgroups nor in the hydrophobic membrane interior. Finally, βAP(1−40) interacts with negatively charged monolayers only at a low packing density of the lipids but not under conditions equivalent to those of a lipid bilayer.

Alzheimer's βAP peptides exhibit only a modest surface activity (*58*). In the case of βAP(1−40), the surface tension of water is reduced linearly from 72 to 60 mN/m up to a peptide concentration of 25 μM. A further increase in peptide concentration does not reduce the surface tension but leads to peptide aggregation (*58*). The rather weak surfactant properties of βAP(1−40) are consistent with the monolayer and NMR data described above.

The present results appear, however, to be in contrast with single channel recordings of βAP(1−40) in model membranes, which provide evidence for ion-selective βAP(1−40) channel (*14*−*16*). For a critical evaluation of these results, it should be noted that the model membranes contained decane and thus were characterized by a considerably softer packing. The monolayer equivalence pressure of such a membrane is distinctly lower than that of a bilayer without organic solvent. Moreover, the peptide was first incorporated into a suspension of pure phosphatidylserine liposomes that were fused with the bilayer upon addition of $CaCl_2$. Thus, a *trans*-membrane orientation of βAP(1−40) cannot be excluded *a priori*, but the insertion appears to require specific catalytic conditions.

Monolayer, NMR, and surface activity studies argue against a spontaneous penetration of βAP(1−40) into the lipid bilayer. On the other hand, conformational changes of βAP(1−40) are observed upon the addition of lipid vesicles and must be caused by peptide−membrane interactions at the bilayer surface. Negatively charged phospholipids are crucial to change the peptide conformation, attesting to a mainly electrostatic interaction between the peptide and the lipid bilayer.

All experiments were performed at physiological pH but at a low ionic strength. At higher NaCl concentrations, the peptide−lipid interactions were found to be screened. The CD experiments are, however, in agreement with recent data of McLaurin and Chakrabartty at pH 6.0 and 120 mM NaCl/50 mM sodium phosphate (*18*). Apparently a small shift in pH is sufficient to increase the electric charge of βAP(1−40) such that electrostatic interactions remain dominant.

Using CD spectroscopy, it is possible to distinguish two well-defined equilibria for human βAP(1−40) upon titration with mixed POPC/POPG (75/25) vesicles. The CD spectra reveal first a random coil $\rightleftarrows$ β-structured aggregate equilibrium that is followed by a transition to an α-helical structure, the latter at a lipid-to-protein ratio >55. The random coil $\rightleftarrows$ β-structure equilibrium has been discussed previously and can be described quantitatively by a cooperative two-state equilibrium (*30*). The lipid-induced β-structure → α-helix transition has not been observed before. If pure POPG vesicles are employed, the β-structure $\rightleftarrows$ α-helix transition occurs already at lower L/P ratios (L/P ∼ 11) and is not clearly separated from the random coil $\rightleftarrows$ β-structure transition.

Helical structures of Alzheimer βAPs or fragments thereof have been produced previously with organic solvents and micellar solutions but not with lipids. NMR measurements of human βAP(1−40) in 40% trifluoroethanol (TFE)/water revealed two short helices, Gln15-Asp23 and Ile31-Met35, whereas the rest of the peptide was in random coil conformation (*24*). Analogous NMR and CD studies on the βAP(1−28) fragment in 60% TFE showed a longer α-helix from Tyr10/Glu11 to Ser26, most probably due to the higher TFE content (*59*, *60*). The fragment βAP(25−35) adopts an essentially α-helical structure (from Lys28 to Leu34) in SDS micelles, again as deduced from NMR spectra (*25*).

The α-helix content induced by negatively charged phospholipid vesicles is smaller than that in 25−50% TFE. Since a penetration of the peptide into the membrane interior can be excluded, the mechanism of helix formation at the membrane surface must be different from that in organic solution and micelles. Helix formation is probably triggered by purely electrostatic interactions since βAP(1−40) carries a total of five positive charges between residues Arg5 and Lys16. In a helical-wheel representation, these are positioned on the same face of the helix, facilitating an optimum electrostatic interaction with the negatively charged membrane. The lipid surface could thus act as a matrix for α-helix formation aligning the cationic side chains of the N-terminal parts of βAP(1−40) in proper order. Since the peptide does not penetrate into the lipid membrane, the helix axis must be oriented essentially parallel to the membrane surface. The C-terminal part retains a nonstructured conformation and does also not intercalate between the lipids.

Surprisingly, the electrostatic interaction between βAP(1−40) and the lipid membrane is not detected with NMR spectroscopy. The behavior of βAP(1−40) parallels that of a small basic peptide pentalysine, Lys_5, which binds to negatively charged membranes by a purely electrostatic mechanism (*61*−*65*). Lys_5 exhibits an apparent partition coefficient of 5×10^4 for membranes containing 20% anionic lipids (*64*), but the quadrupole splittings of the phosphocholine headgroup are not at all changed (*56*). Based on deuterium NMR (*56*) and high-pressure fluorescence studies (*64*), it was thus concluded that Lys_5 binds only to the outer envelope of the lipid headgroups. A similar binding site can be envisaged for βAP(1−40). The α-helical part of βAP(1−40) must be positioned at the periphery of the lipid headgroup layer in order to avoid a conformational change of the lipid headgroups.

The peptide fragment βAP(25−35) exhibits sequence homologies with neuropeptides of the tachykinin family such as substance P (SP) (*66*, *67*). Interestingly, SP and its agonist (Nle^9)SP exhibit a similar physical−chemical behavior as βAP(1−40) in the presence of lipid membranes. SP and (Nle^9)SP do not penetrate into neutral POPC bilayers or into POPC monolayers at high lateral pressure (*36*). However, in the presence of negatively charged POPG vesicles, both peptides undergo a concentration-dependent conformational change. At a low L/P ratio (<30), the β-sheet structure is predominant. At high lipid-to-protein ratios (>40), both peptides adopt the helix conformation.

The functional role of α-helical βAP(1−40) is not known. Using an *in vitro* plaque growth assay, the structure of several βAP fragments was correlated with their functional properties (*27*, *68*). The fragment βAP(10−35) NH_2 displays the same activity in plaque growth as βAP(1−40) and is sufficiently soluble in water for NMR spectroscopy. The plaque competent conformation of βAP(10−35) was not helical but folded (*27*). By analogy, it is suggested that the active form of βAP(1−40) is also not helical. In a different *in vitro* assay, we have shown recently that β-structured βAP(1−

40) is toxic and that toxicity can be inhibited by molecules with a large dipole moment (*69*).

From a theoretical point of view, α-helix formation of βAP(1−40) at the membrane surface may be considered as an alternative mechanism in protein folding, different from the prevailing model of folding proteins *into* membranes (*70*−*72*). In this latter model, the protein partitions into the lipid water interface, i.e., a layer of reduced dielectric constant, where it forms a helical structure by hydrogen bonding within the peptide backbone and may finally achieve a transbilayer orientation (*73*). In the case of βAP(1−40), the experimental evidence argues against membrane penetration. The electrostatic restriction of the charged peptide residues to the outer boundary of the lipid membrane appears to be sufficient to initiate the process of intramolecular hydrogen bond formation and helix formation.

REFERENCES

1. Iversen, L. L., Mortishire-Smith, R. J., Pollack, S. J., and Shearman, M. S. (1995) *Biochem. J. 311*, 1−16.
2. Selkoe, D. J. (1991) *Neuron 6*, 487−498.
3. Selkoe, D. J. (1994) *Curr. Opin. Neurobiol. 4*, 708−716.
4. Seubert, P., Vigo-Pelfry, C., Esch, F., Lee, M., Dovey, H., Davis, D., Sinha, S., Schlossmacher, M., Whaley, J., Swindelhurst, C., McCormack, R., Wolfert, R., Selkoe, D., Lieberburg, I., and Schenk, D. (1992) *Nature 359*, 325−327.
5. Shoji, M., Golde, T. E., Ghiso, J., Cheung, T. T., Estus, S., Shaffer, L. M., Cai, X.-D., McKay, D. M., Tintner, R., Frangione, B., and Younkin, S. G. (1992) *Science 258*, 126−129.
6. van Gool, W. A., Kuiper, M. A., Walstra, G. J. M., Wolters, E. Ch., and Bolhuis, P. A. (1994) *Annu. Neurol. 37*, 277−279.
7. Pike, C. J., Burdick, D, Walencewicz, A. J., Glabe, C. G., and Cotman, C. W. (1993) *J. Neurosci. 13*, 1676−1687.
8. Simmons, L. D., May, P. C., Tomaselli, K. J., Rydel, R. E., Fuson, K. S., Brigham, E. F., Wright, S., Lieberburg, I., Becker, G. W., Brems, D. N., and Ying Li, W. (1994). *Mol. Pharmacol. 45*, 373−379.
9. Ueda, K., Fukui, Y., and Kageyama, H. (1994) *Brain Res. 639*, 240−244.
10. Joslin, G., Krause, J. E., Hershey, A. D., Adams, S. P., Fallon, R. J., and Perlmutter, D. H. (1991) *J. Biol. Chem. 266*, 21897−21902.
11. Boland, K., Behrens, M., Choi, D., Manias, K., and Perlmutter, D. H. (1996) *J. Biol. Chem. 271*, 18032−18044.
12. Shimohigashi, Y., Matsumoto, H., Takano, Y., Saito, R., Iwata, T., Kamiya, H.-O., and Ohno, M. (1993) *Biochem. Biophys. Res. Commun. 193*, 624−630.
13. Rovero, P., Patacchini, R., Renzetti, A. R., Brown, M., Mizrahi, J., Maggi, C. A., and Giachetti, A. (1992) *Neuropeptides 22*, 99−101.
14. Arispe, N., Pollard, H. B., and Rojas, E. (1993) *Proc. Natl. Acad. Sci. U.S.A. 90*, 10573−10577.
15. Arispe, N., Rojas, E., and Pollard, H. B. (1993) *Proc. Natl. Acad. Sci. U.S.A. 90*, 567−571.
16. Durell, S. R., Guy, H. R., Arispe, N., Rojas, E., and Pollard, H. B. (1994) *Biophys. J. 67*, 2137−2145.
17. McLaurin, J., and Chakrabartty, A. (1996) *J. Biol. Chem. 271*, 26482−26489.
18. McLaurin, J., and Chakrabartty, A. (1997) *Eur. J. Biochem. 245*, 355−363.
19. Pillot, T., Goethals, M., Vanloo, B., Talussot, C., Brasseur, R., Vandekerckhove, J., Rosseneu, M., and Lins, L. (1996) *J. Biol. Chem. 271*, 28757−28765.
20. Lansbury, P. T., Jr. (1992) *Biochemistry 31*, 6865−6869.
21. Inouye, H., Fraser, P. E., and Kirschner, D. A. (1993) *Biophys. J. 64*, 502−519.
22. Spencer, R. G., Halverson, K. J., McDermott, A. E., Griffin, R. G., and Lansbury, P. T., Jr. (1991) *Biochemistry 30*, 10382−10387.
23. Barrow, C. J., and Zagorski, M. G. (1991) *Science 253*, 180−182.
24. Sticht, H., Bayer, P., Willbold, D., Dames, S., Hilbich, C., Beyreuther, K., Frank, R. W., and Rösch, P. (1995) *Eur. J. Biochem. 233*, 293−298.
25. Kohno, T., Kobayashi, K., Maeda, T., Sato, K., and Takashima, A. (1996) *Biochemistry 35*, 16094−16104.
26. Mason, R. P., Estermyer, J. D., Kelly, J. F., and Mason, P. E. (1996) *Biochem. Biophys. Res. Commun. 222*, 78−82.
27. Lee, J. P., Stimson, E. R., Ghilardi, J. R., Mantyh, P. W., Lu, Y.-A., Felix, A. M., Llanos, W., Behbin, A., Cummings, M., Van Criekinge, M., Timms, W., and Maggio, J. E. (1995) *Biochemistry 34*, 5191−5200.
28. Terzi, E., Hölzemann, G., and Seelig, J. (1994) *Biochemistry 33*, 1345−1350.
29. Terzi, E., Hölzemann, G., and Seelig, J. (1994) *Biochemistry 33*, 7434−7441.
30. Terzi, E., Hölzemann, G., and Seelig, J. (1995) *J. Mol. Biol. 252*, 633−642.
31. Tamm, L. K., and Seelig, J. (1983) *Biochemistry 22*, 1474−1483.
32. Seelig, J., and Waespe-Sarcevic, N. (1978) *Biochemistry 17*, 3310−3315.
33. Yang, J. T., Wu, C.-S. C., and Martinez, H. M. (1986) *Methods Enzymol. 130*, 208−269.
34. Fromherz, P. (1975) *Rev. Sci. Instrum. 46*, 1380−1385.
35. Hanakam, F., Gerisch, G., Lotz, S., Alt, T., and Seelig, A. (1996) *Biochemistry 35*, 11036−11044.
36. Seelig, A., Alt, T., Lotz, S., and Hölzemann, G. (1996) *Biochemistry 35*, 4365−4374.
37. Seelig, A. (1987) *Biochim. Biophys. Acta 899*, 196−204.
38. Seelig, A., and Macdonald, P. M. (1989) *Biochemistry 28*, 2490−2496.
39. Otvos, L., Jr., Szendrei, G. I., Lee, V. M.-Y., and Mantsch, H. H. (1993) *Eur. J. Biochem. 211*, 249−257.
40. Niederberger, W., and Seelig, J. (1976) *J. Am. Chem. Soc. 98*, 3704−3706.
41. Seelig J. (1978) *Biochim. Biophys. Acta 505*, 105−141.
42. Seelig, J. (1977) *Q. Rev. Biophys. 10*, 353−418.
43. Brown, M. F., and Seelig, J. (1978) *Biochemistry 17*, 381−384.
44. Akutsu, H., and Seelig, J. (1981) *Biochemistry 20*, 7366−7373.
45. Macdonald, P. M., and Seelig, J. (1988) *Biochemistry 27*, 6769−6775.
46. Boulanger, Y., Schreier, S., and Smith, I. C. P. (1981) *Biochemistry 20*, 6824−6830.
47. Seelig, A., Allegrini, P. R., and Seelig, J. (1988) *Biochim. Biophys. Acta 939*, 267−276.
48. Bäuerle, H.-D., and Seelig, J. (1991) *Biochemistry 30*, 7203−7211.
49. Sixl, F., and Watts, A. (1983) *Proc. Natl. Acad. Sci. U.S.A. 80*, 1613−1615.
50. Scherer, P. G., and Seelig, J. (1987) *EMBO J. 6*, 2915−2922.
51. Scherer, P. G., and Seelig, J. (1989) *Biochemistry 28*, 7720−7728.
52. Kuchinka, E., and Seelig, J. (1989) *Biochemistry 28*, 4216−4221.
53. Beschiaschvili, G., and Seelig, J. (1990) *Biochemistry 29*, 52−58.
54. Spühler, P., Anantharamaiah, G. M., Segrest, J. P., and Seelig, J. (1994) *J. Biol. Chem. 269*, 23904−23910.
55. Seelig, J., Macdonald, P. M., and Scherer, P. G. (1987) *Biochemistry 26*, 7535−7541.
56. Roux, M., Neumann, J. M., Bloom, M., and Devaux, P. F. (1988) *Eur. Biophys. J. 16*, 267−273.
57. Habiger, R. G. K., Cassal, J. M., Kempen, H. J. M., and Seelig, J. (1992) *Biochim. Biophys. Acta 1103*, 69−76.
58. Soreghan, B., Kosmoski, J., and Glabe, C. (1994) *J. Biol. Chem. 269*, 28551−28554.
59. Zagorski, M. G., and Barrow, C. J. (1992) *Biochemistry 31*, 5621−5631.
60. Talafous, J., Marcinowski, K. J., Klopman, G., and Zagorski, M. G. (1994) *Biochemistry 33*, 7788−7796.
61. Kim, J., Mosior, M., Chung, L. A., Wu, H., and McLaughlin, S. (1991) *Biophys. J. 60*, 135−148.

62. Mosior, M., and McLaughlin, S. (1992) *Biochemistry 31,* 1767−1773.
63. Mosior, M., and McLaughlin, S. (1992) *Biochim. Biophys. Acta. 1105,* 185−187.
64. Montich, G., Scarlata, S., McLaughlin, S., Lehrmann, R., and Seelig, J. (1993) *Biochim. Biophys. Acta. 1146,* 17−24.
65. Ben-Tal, N., Honig, B., Peitzsch, R. M., Denisov, G., and McLaughlin, S. (1996) *Biophys. J. 71,* 561−575.
66. Masters, C. L., Simms, G., Weinman, N. A., Multhaup, G., McDonald, B. L., and Beyreuther, K. (1985) *Proc. Natl. Acad. Sci. U.S.A. 82,* 4245−4249.
67. Yankner, B. A., Duffy, L. K., and Kirschner, D. A. (1990) *Science 250,* 279−282.
68. Esler, W. P., Stimson, E. R., Ghilardi, J. R., Lu, Y.-A., Felix, A. M., Vinters, H. V., Mantyh, P. W., Lee, J. P., and Maggio, J. E. (1996) *Biochemistry 35,* 13914−13921.
69. Hertel C., Terzi, E., Hauser, N., Jakob-Røtne, R., Seelig, J., and Kemp, J. A. (1997) *Proc. Natl. Acad. Sci. U.S.A. 94,* 9412−9416.
70. Wimley, W. C., and White, S. H. (1996) *Nat. Struct. Biol. 3,* 842−848.
71. Deber, C. M., and Goto, N. K. (1996) *Nat. Struct. Biol. 3,* 815−818.
72. Engelman, D. M. (1996) *Science 274,* 1850−1851.
73. Liu, L.-P., and Deber, C. M. (1997) *Biochemistry 36,* 5476−5482.

BI971843E